

# Modeling and analysis of chlorine dioxide, chlorite, and chlorate propagation in a drinking water distribution system

Sabrina Sorlini, Michela Biasibetti, Francesca Gialdini  
and Alessandro Muraca

## ABSTRACT

The drinking water distribution system of Cremona, in the north of Italy, was monitored for 6 years (2006–2011) analyzing chlorine dioxide, chlorite, and chlorate concentrations. The software Epanet 2.0 (USEPA) was applied to the distribution system. The mixing zone of the water coming from the two drinking water treatment plants, respectively located to the west and east of the city, was estimated using the software. Propagation of chlorine dioxide, chlorite, and chlorate was simulated with the software. Measured and simulated results were compared. The results of the distribution system monitoring showed a high chlorine dioxide consumption, since residual chlorine concentration was always below  $0.12 \text{ mg L}^{-1}$ . Chlorite concentration was over  $700 \text{ } \mu\text{g L}^{-1}$  for 12–16% of results in the first 2 years, for 48% of results in 2008, and for 1–8% of results from 2009 to 2011. In particular, chlorite exceeded  $700 \text{ } \mu\text{g L}^{-1}$  at points of the network more distant from the treatment plants. Conversely, chlorate concentration was always below  $200 \text{ } \mu\text{g L}^{-1}$ . The mixing zone of the water in the distribution system was determined, and the comparison between measured and simulated concentrations showed the usefulness of the model for predicting disinfectant and by-product propagation in the distribution system.

**Key words** | chlorate, chlorine dioxide, chlorite, drinking water, modeling, water distribution system

Sabrina Sorlini (corresponding author)  
Michela Biasibetti  
Francesca Gialdini  
Alessandro Muraca  
Department of Civil Engineering, Architecture,  
Land, Environment and of Mathematics,  
University of Brescia,  
via Branze 43,  
Brescia 25123,  
Italy  
E-mail: [sabrina.sorlini@unibs.it](mailto:sabrina.sorlini@unibs.it)

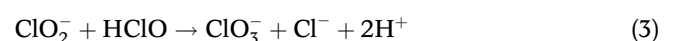
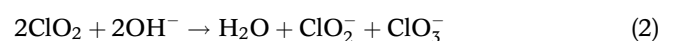
Michela Biasibetti  
Department of Civil Engineering and Architecture,  
University of Pavia,  
Via Ferrata, 1,  
Pavia 27100,  
Italy

## INTRODUCTION

Disinfection is applied in drinking water treatment plants (DWTPs) to ensure water quality and to avoid bacterial contamination in drinking water distribution systems (DWDSs). However, disinfectant concentration in DWDSs decreases with time, while disinfection by-product (DBP) formation increases; this is due to chemical reactions of the disinfectant with dissolved and particulate matter in water, biofilm, and pipe wall material (Wable *et al.* 1991; Zhang *et al.* 1992; Ki  n   *et al.* 1998; Al-Jasser 2007).

If chlorine dioxide ( $\text{ClO}_2$ ) is used as a disinfectant, chlorite ( $\text{ClO}_2^-$ ) and chlorate ( $\text{ClO}_3^-$ ) can be produced as DBPs. In fact,  $\text{ClO}_2^-$  and  $\text{ClO}_3^-$  can be produced during the  $\text{ClO}_2$  generation process in the DWTP (Equations (1) and (2)), during

water treatment and in the DWDS. Concerning the  $\text{ClO}_2$  generation process in DWTPs,  $\text{ClO}_2^-$  can be used as a reagent to produce  $\text{ClO}_2$  in DWTPs. In particular,  $\text{ClO}_2$  can be generated by  $\text{ClO}_2^-$  oxidation with chlorine. Moreover,  $\text{ClO}_2^-$  and  $\text{ClO}_3^-$  can be produced from the interaction between  $\text{ClO}_2$  and hypochlorite ( $\text{OCl}^-$ ) (Equation (3)) (Gates *et al.* 2009):



During water treatment,  $\text{ClO}_2$  can react with natural organic matter (NOM) in water, producing  $\text{ClO}_2^-$  and  $\text{ClO}_3^-$ . The main parameters that influence  $\text{ClO}_2^-$  and  $\text{ClO}_3^-$  formation are water quality parameters such as pH, temperature, and NOM content, and operating conditions such as the disinfectant dosage (Korn *et al.* 2002). In particular, studies showed that  $\text{ClO}_2$  concentration, temperature, and NOM content are the most significant parameters influencing  $\text{ClO}_2^-$  and  $\text{ClO}_3^-$  formation (Korn *et al.* 2002; Collivignarelli & Sorlini 2004; Gates *et al.* 2009).

In DWDSs,  $\text{ClO}_2$  can still react with organic and inorganic compounds, degrading  $\text{ClO}_2^-$ ,  $\text{ClO}_3^-$ , and chloride ( $\text{Cl}^-$ ) as a consequence of reactions in pipes and tanks (Baribeau *et al.* 2002). Studies showed that iron corrosion scales in DWDS pipes generally contain reduced iron, which can react with oxidative disinfectants (Sarin *et al.* 2001, 2004a, 2004b) such as  $\text{ClO}_2$ , with undesirable losses in the disinfectant residual (Zhang *et al.* 2008).

The main factors that can influence  $\text{ClO}_2^-$  and  $\text{ClO}_3^-$  formation in a DWDS are the  $\text{ClO}_2$  residual concentration, pipe material and diameter, corrosion by-products and biofilm, water residence time and water temperature. Concerning the fate of  $\text{ClO}_2$  and its DBPs in DWDSs, some researchers found that  $\text{ClO}_2$  concentration decreases with increasing residence time (Olivieri *et al.* 1986; Thompson 1988). Concerning corrosion by-products and biofilm, the reaction between  $\text{ClO}_2^-$  and  $\text{Fe}^{2+}$ , which is the main corrosion by-product in metallic pipes, leads to a  $\text{ClO}_2^-$  decrease (Zhang *et al.* 2008). Moreover,  $\text{ClO}_2^-$  decreases with increasing water residence time in DWDSs, while  $\text{ClO}_3^-$  increases or remains stable (Thompson 1988; McGuire *et al.* 1990; Lafrance *et al.* 1992).

Therefore, it is important to evaluate spatial and temporal variation in residual chlorine, chlorite ( $\text{ClO}_2^-$ ), and chlorate ( $\text{ClO}_3^-$ ) within DWDSs. In fact, the World Health Organization (WHO) recommends a free residual chlorine concentration of  $0.2 \text{ mg L}^{-1}$  in DWDSs (WHO 2011); moreover, since  $\text{ClO}_2^-$  and  $\text{ClO}_3^-$  can cause oxidative damage to human red blood cells, each compound should not exceed the WHO guideline value (GV) of  $700 \mu\text{g L}^{-1}$  in drinking water (WHO 2011). The Italian regulation limit exists only for  $\text{ClO}_2^-$  ( $700 \mu\text{g L}^{-1}$ ), while  $\text{ClO}_3^-$  is not regulated (Italian Legislative Decree 31/2001).

Prediction of the disinfectant residual and DBP propagation in a DWDS can be achieved using water

distribution modeling (WDM), which allows simulation and evaluation of a DWDS under different operating conditions. For example, the software Epanet 2.0 is a WDM in the public domain, developed by the United States Environmental Protection Agency (USEPA), which models the hydraulic and water quality behavior of water distribution piping systems (Rossman 2000).

In the literature, several studies are available on the measurement and modeling of chlorine and chlorate in DWDSs (Clark *et al.* 1994; Rossman *et al.* 1994; Islam *et al.* 1997; Rodriguez & Sérodes 1998, 2001; Li & Zhao 2006; Al-Jasser 2007; Curtis *et al.* 2009; Mohamed & Abozeid 2011; Boano *et al.* 2016). Some researchers modeled chlorine residual propagation in DWDSs with the Epanet software and obtained good agreement with observed chlorine levels at locations where the hydraulics were well characterized (Rossman *et al.* 1994). Other researchers studied the chlorine residual propagation in DWDSs and found that residuals varied widely both spatially and temporally; moreover, they observed that long residence times in storage tanks caused low or nonexistent residual disinfectant concentrations in the DWDS; further, they found that supply system operation has a significant effect on the distribution and concentration of chlorine residuals in the DWDS (Clark *et al.* 1993). Since chlorine is the most popular and traditional disinfectant, most modeling efforts have been focused on trihalomethanes (THMs) (Sadiq & Rodriguez 2004). Some researchers studied THM reaction kinetics and developed a model for predicting their formation in DWDSs. They found that a second-order reaction is a good predictor of THM formation, and they observed good agreement between calculated and measured values, confirming that the model is applicable to an actual DWDS (Li & Zhao 2006). However, since few studies are available on  $\text{ClO}_2$ ,  $\text{ClO}_2^-$ , and  $\text{ClO}_3^-$  propagation in DWDSs by means of WDM, the kinetic reactions of  $\text{ClO}_2$ ,  $\text{ClO}_2^-$ , and  $\text{ClO}_3^-$  and the simulation of their propagation in DWDSs by means of WDM must be further investigated.

This novel work is aimed at understanding  $\text{ClO}_2$ ,  $\text{ClO}_2^-$ , and  $\text{ClO}_3^-$  propagation in a DWDS by means of WDM software. It studies the DWDS of Cremona, in the north of Italy, fed by two treatment plants in which  $\text{ClO}_2$  disinfection is applied, respectively located to the west and east of the city. The DWDS was monitored for 6 years (2006–2011)

analyzing residual chlorine,  $\text{ClO}_2^-$ , and  $\text{ClO}_3^-$  concentrations at 26 points of the network. The Epanet 2.0 software (USEPA) was applied to the DWDS in order to estimate the mixing zone of the water coming from the west and east treatment plants, and in order to simulate the propagation of  $\text{ClO}_2$ ,  $\text{ClO}_2^-$ , and  $\text{ClO}_3^-$ . The measured and simulated results were compared in order to evaluate the applicability of the model to the DWDS.

## MATERIAL AND METHODS

### Drinking water supply system of Cremona (Italy)

The drinking water supply system studied is located in the city of Cremona (76,000 inhabitants), in the north of Italy. Groundwater is withdrawn by two well fields, respectively consisting of nine wells and ten wells, and respectively located in the north-west and east of the city; each well field is capable of providing a maximum flow rate of  $38.9 \text{ ML d}^{-1}$  and each well withdraws water at a depth between 160 and 200 m. Groundwater contains methane ( $\text{CH}_4$ ), hydrogen sulfide ( $\text{H}_2\text{S}$ ), ammonia ( $\text{NH}_4^+$ ), iron (Fe), manganese (Mn), and arsenic As(III). The main raw water quality characteristics (average values) are:  $\text{CH}_4$   $5 \text{ mg L}^{-1}$ ,  $\text{H}_2\text{S}$   $0.15 \text{ mg L}^{-1}$ ,  $\text{NH}_4^+$   $1.4 \text{ mg L}^{-1}$ , Fe  $57 \text{ } \mu\text{g L}^{-1}$ , Mn  $51 \text{ } \mu\text{g L}^{-1}$ , As  $15 \text{ } \mu\text{g L}^{-1}$ , pH 8.0, temperature  $17^\circ\text{C}$ , Kubel index  $2.5 \text{ mgO}_2 \text{ L}^{-1}$ , bromide  $<0.005 \text{ mg L}^{-1}$ , ultraviolet absorption at 254 nm ( $\text{UV}_{254}$ )  $0.0786 \text{ cm}^{-1}$ , and TOC  $4.10 \text{ mg L}^{-1}$ . The well fields feed two equal DWTPs, respectively located to the east and west of the city, each using the following treatment train: aeration, biofiltration, chemical oxidation with potassium permanganate and coagulation with ferric chloride, sand filtration, and final disinfection with  $\text{ClO}_2$ . The disinfectant dosage is  $0.8 \text{ mg ClO}_2 \text{ L}^{-1}$  ( $0.42 \text{ mg Cl}_2 \text{ L}^{-1}$ ) in each DWTP. After treatment, water is supplied to the DWDS by means of pumps with inverters. The east DWTP has three output sections, and the west DWTP has five output sections. The east DWTP supplies a reservoir located in the center of the city, after which a pumping station delivers water to the city. The pumping station has two output sections.

The DWDS is 259 km in length, 65% of the pipes are steel, 19% cast iron, 6% HDPE (high-density polyethylene), 10% other materials, and the diameters vary from approximately 60 to 800 mm.

### Evaluation of the disinfectant and DBP concentrations in the distribution system

Data of the residual  $\text{Cl}_2$ ,  $\text{ClO}_2^-$ , and  $\text{ClO}_3^-$  concentrations measured at 26 points of the DWDS (Figure 1) from 2006 to 2011 (monthly) were collected in order to evaluate the disinfectant and DBP concentrations in the DWDS.

### Modeling of the drinking water supply system

#### Model development

The model of the DWDS was developed with the USEPA software, Epanet 2.0. According to the DWDS cartography, the altimetry of each junction and the length, material, and roughness coefficient of each pipe were inserted in the software model. The modeled DWDS was simplified in order to simulate only a part of the system, and pipes below 150 mm were not considered. However, the discharge related to each removed part of the system was inserted into the appropriate junction in the model (see 'Development of the hydraulic model'). The simplified scheme, characterized by five closed paths, 144 junctions, and a 23 km total length, was used for all the subsequent simulations (Figure 2).

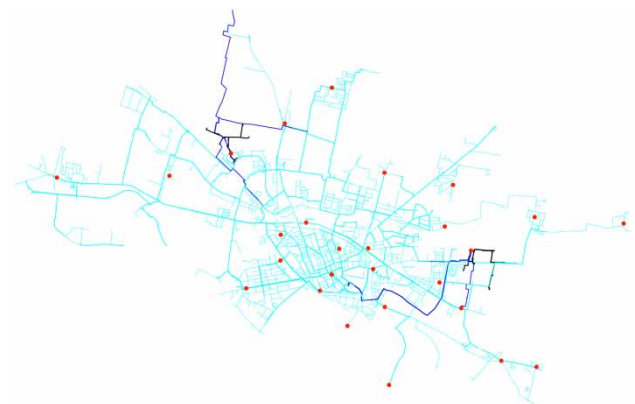
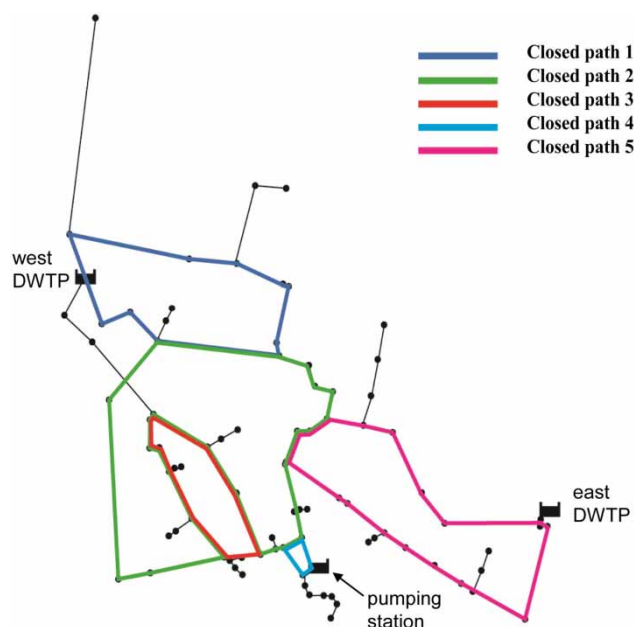


Figure 1 | Sampling points in the DWDS.



**Figure 2** | Simplified scheme of the DWDS of Cremona (Italy) used for the simulations.

*Development of the hydraulic model.* In order to develop the hydraulic model, the daily trends of pressure and discharge in the DWDS were analyzed. These trends were elaborated using pressure and discharge values measured at the outlet of each DWTP and at the outlet of the pumping station located in the city center (Figure 3). The average pressure and discharge values were calculated from these trends (at each output section: average daily discharge ranges from 17 to 50 L/s and average daily pressure varies from 3.8 to 5.1 bar) and, then, used in the model. Since all the pumps at the outlet of the DWTPs and the pumping station are equipped with inverters, pressure and discharge are controlled at the output section (pump head and related discharge are managed and regulated). Pumping operating point is regulated as time function. Therefore, to simulate this behavior, pressure reduction valves and discharge reduction valves were inserted in the model at the junctions downstream of each pump; the measured average pressure and discharge values were inserted in these valves in the model at the output section of the DWTPs and the pumping station.

The users of the DWDS are 84% civil, 15% industrial, and 1% public. In the DWDS, time varying demand was implemented using direct discharge metering at all users for each category. Therefore, each junction has a certain water

demand. Temporal variation in water demand at each junction depends on users' number and related category. Furthermore, water demands higher than 10,000  $\text{m}^3/\text{year}$  (industries) were concentrated in a single junction of the model. The total water demand of the removed zone was considered located in a single junction of the model.

In order to model the daily water discharge at different points of the DWDS, the daily trend of the discharge in each junction was estimated considering 154 users/km, a total delivered water volume of about 7,800,000  $\text{m}^3$ , and a 32% distribution loss. Different hourly coefficients were applied to the daily average discharge measured at the output section of the two DWTPs and the pumping station (Figure 4(a)–4(c)). Different hourly coefficients were applied to the daily average discharge of industries located at different points of the DWDS (Figure 4(d)). Therefore, the demand pattern (daily water discharge trend) was inserted at each junction in the modeled DWDS (Figure 5).

*Modeling the water mixing zone.* The chemical validation of the model was carried out in order to determine the water mixing zone in the DWDS and to simulate the disinfectant and DBP propagation in the DWDS.

In order to determine the mixing zone of the water coming from the two DWTPs, the propagation of a salt in the modeled system was simulated with the software Epanet 2.0. The aim was to evaluate the propagation in the system of a substance without decay or growth. The initial salt concentration in the water was considered zero. A salt concentration of 70,000  $\text{mg L}^{-1}$ , twice that of seawater, was dosed in the model continuously for 24 hours, at first only in the east DWTP and in the central pumping station and then only in the west DWTP. The salt concentration in the junctions of the modeled system was evaluated. In particular, in the case where salt was dosed only in the east DWTP and pumping station, the salt propagation was evaluated during 24 h simulation. The pipes in which salt was never detected in 24 h and the pipes located farthest from the east DWTP and from the pumping station in which salt concentration was diverse from zero at a certain time of the day were determined. The same evaluation was carried out in the case where salt was dosed in the west DWTP. In particular, the water mixing zone was defined as the modeled DWDS zone constituted by the pipes where a salt concentration diverse from

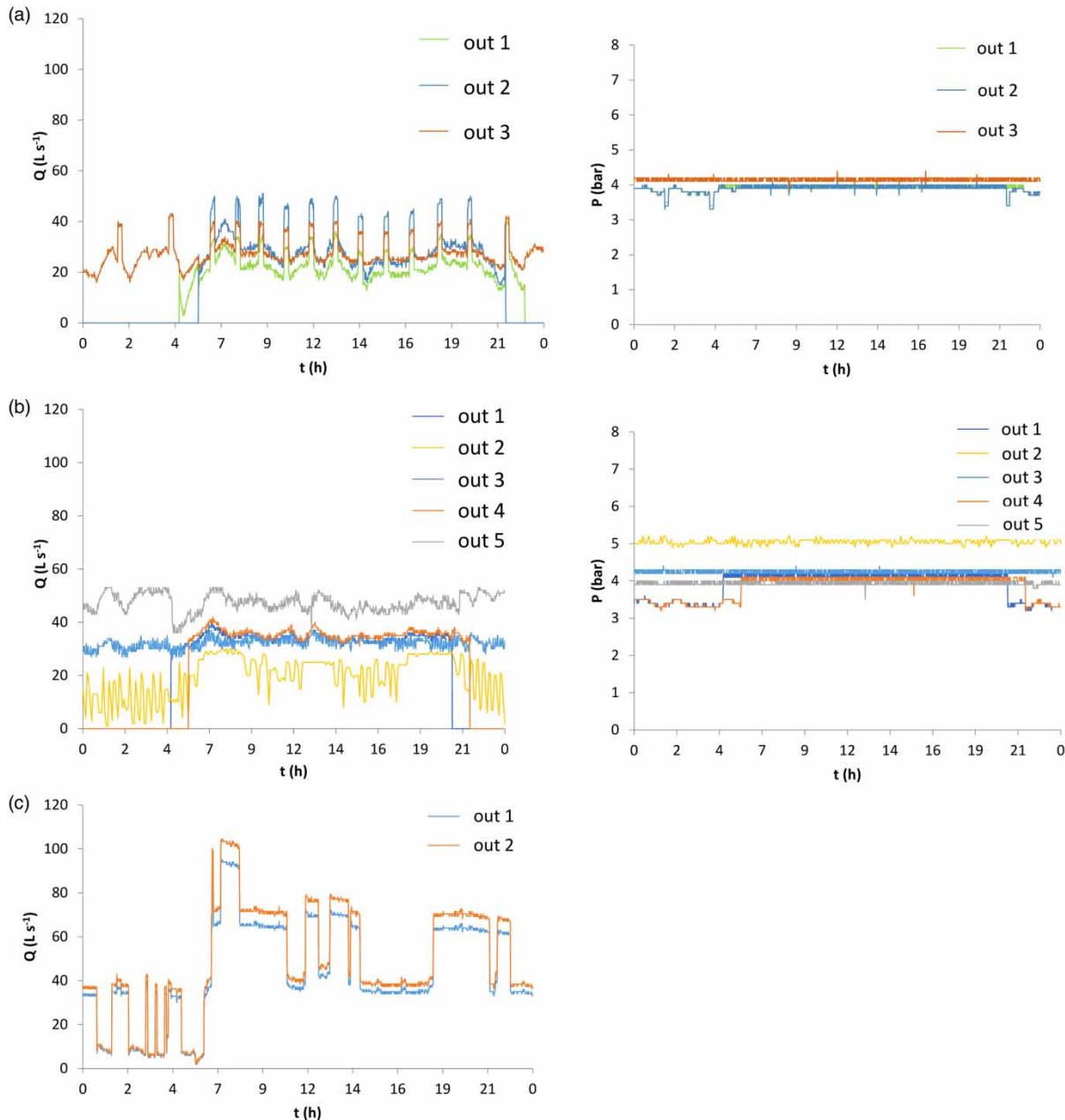


**Figure 3** | Daily pressure and discharge trends measured at the three output sections of the east DWTP (a), at the five output sections of the west DWTP (b), and at the two output sections of the pumping station (c).

zero was observed during the 24 h simulation in both cases, dosing salt in the east and the west DWTP, at certain times of the day.

**Chemical validation.** In order to simulate the disinfectant and DBP propagation in the DWDS, the  $\text{ClO}_2$ ,  $\text{ClO}_2^-$ , and  $\text{ClO}_3^-$  reaction kinetics were studied at laboratory scale.

Batch experiments were carried out by treating water samples collected at the outlet of the sand filter of the full-scale DWTP with  $\text{ClO}_2$ . Each 2 L water sample was divided into smaller samples of 100 mL. Each water sample was put in a graduated cylinder and treated with 5 mg L<sup>-1</sup> of  $\text{ClO}_2$ . The  $\text{ClO}_2$  dosage is higher than the one employed in the DWTP final disinfection, because

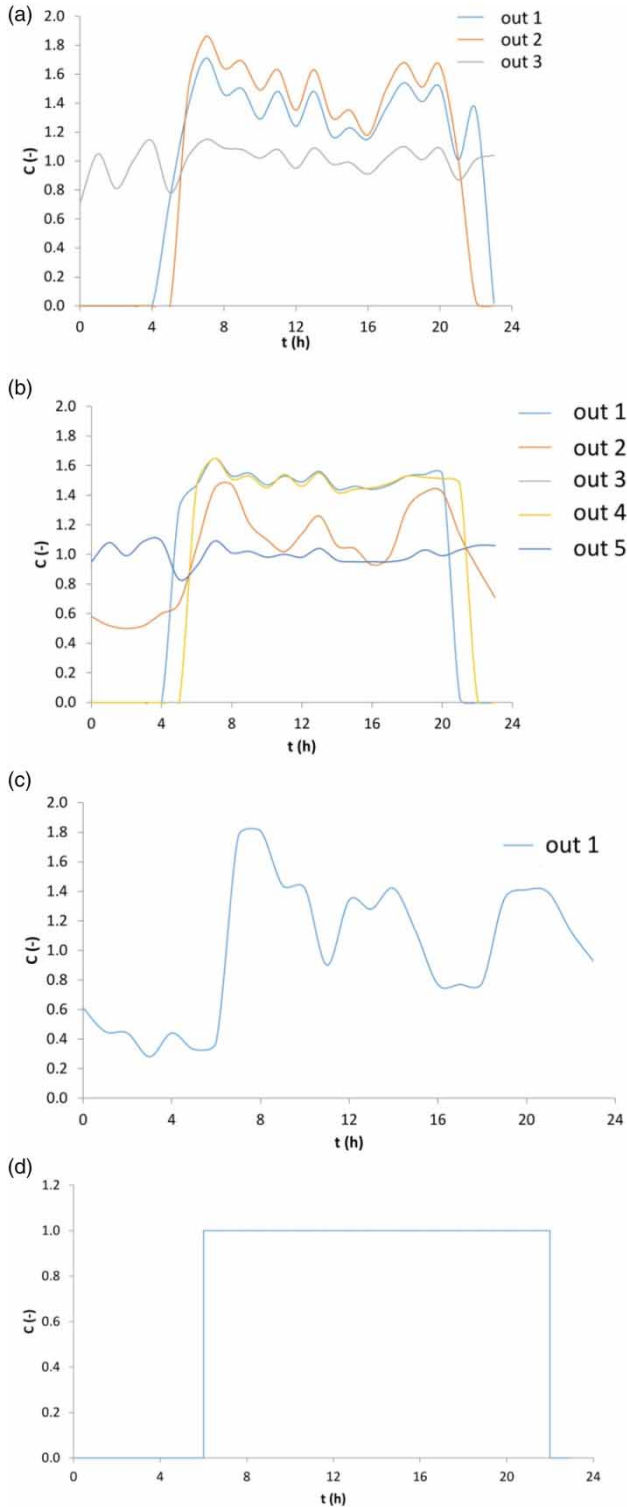


**Figure 4** | Hourly coefficients applied to the daily average discharge at the three output sections of the east DWTP (a), at the five output sections of the west DWTP (b), at the output of the pumping station (c), and for industries located in different points of the DWDS (d).

the aim of this test was to evaluate the ClO<sub>2</sub> consumption and the DBP formation in the presence of a residual ClO<sub>2</sub> concentration. Then, each cylinder was plugged, manually stirred to homogenize the solution and kept in dark conditions. The residual ClO<sub>2</sub>, ClO<sub>2</sub><sup>-</sup>, and ClO<sub>3</sub><sup>-</sup> concentrations were analyzed after 0, 4, 10, 30, 60, 79, 120, 160, 180, 360, 670, 1,440, and 2,280 minutes water-disinfectant contact time. Tests were carried out at a temperature of 22–24 °C and pH 8.0. Water samples were stored in a fridge at 4 °C in dark conditions. The ClO<sub>2</sub> solution (concentration of 250 mgClO<sub>2</sub>/L) was directly collected from the ClO<sub>2</sub> generator used in the DWTP and it was stored in a fridge at 4 °C in dark conditions before use.

The interpolation of the residual concentrations versus time allowed determining the order of each reaction kinetic and the bulk reaction coefficient ( $k_b$ ) for ClO<sub>2</sub>, ClO<sub>2</sub><sup>-</sup>, and ClO<sub>3</sub><sup>-</sup>. The reaction kinetic for ClO<sub>2</sub> is described by a first-order reaction:

$$C = C_0 \cdot e^{k_b t}, \quad k_b < 0$$

$C$  = concentration at  $t$  time (mg L<sup>-1</sup>);  $C_0$  = initial concentration (1 mg L<sup>-1</sup>);  $k_b$  = bulk reaction coefficient (1 s<sup>-1</sup>);  $t$  = contact time (s).

The reaction kinetics for ClO<sub>2</sub><sup>-</sup> and ClO<sub>3</sub><sup>-</sup> are described by zero order reactions:

$$C = C_0 + k_b t, \quad k_b > 0$$

The ln(residual ClO<sub>2</sub>) versus time determined by batch experiments at laboratory scale is shown in Figure 6(a). The exponential function well approximates the distribution of the residual ClO<sub>2</sub> concentrations, with a correlation close to 80%. Therefore, the first-order equation showed a linear ClO<sub>2</sub> decay versus time and  $k_b$  was equal to  $-0.0002 \text{ min}^{-1}$ , thus  $-0.288 \text{ d}^{-1}$ .

The ClO<sub>2</sub><sup>-</sup> and ClO<sub>3</sub><sup>-</sup> concentrations versus time determined by batch experiments at laboratory scale are shown, respectively, in Figure 6(b) and 6(c). The linear function well approximates both the distributions of the ClO<sub>2</sub><sup>-</sup> and ClO<sub>3</sub><sup>-</sup> concentrations, with a correlation close to 80% in both cases. Therefore, the zero-order equation represented both the ClO<sub>2</sub><sup>-</sup> and ClO<sub>3</sub><sup>-</sup> growth versus time,

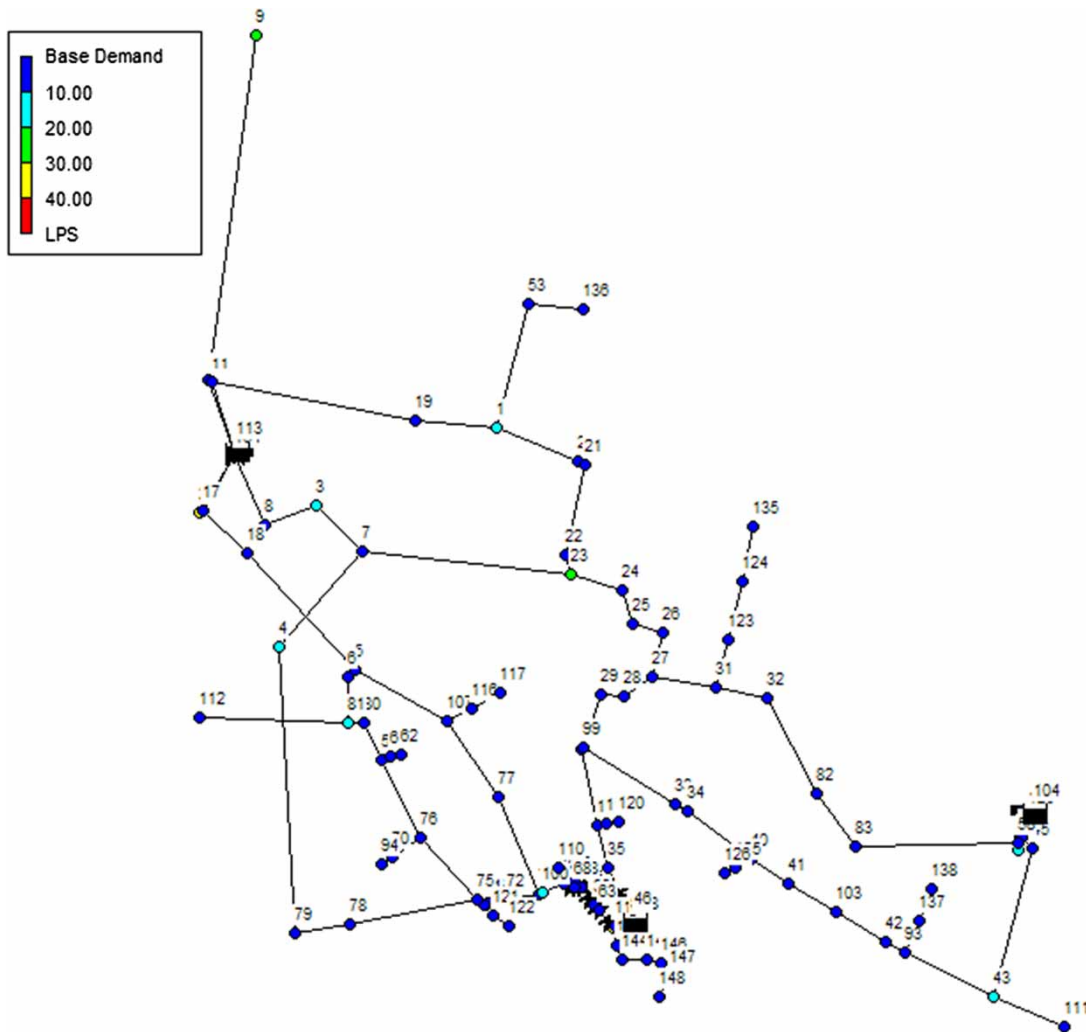


**Figure 5** | Water demand ( $\text{L s}^{-1}$ ) at each numbered junction of the modeled DWDS.

and  $k_b$  was respectively equal to  $0.0004 \text{ mg L}^{-1} \text{ min}^{-1}$ , thus  $0.576 \text{ mg L}^{-1} \text{ d}^{-1}$ , and  $0.00007 \text{ mg L}^{-1} \text{ min}^{-1}$ , thus  $0.101 \text{ mg L}^{-1} \text{ d}^{-1}$ .

In the model, initial  $\text{Cl}_2$ ,  $\text{ClO}_2^-$ , and  $\text{ClO}_3^-$  concentrations at the DWTPs and at the pumping station were the average annual concentrations measured in the real system at these points. In particular, in the model, the initial concentration of residual  $\text{Cl}_2$  was  $0.42 \text{ mg L}^{-1}$  and  $0.02 \text{ mg L}^{-1}$ , respectively, at the outlet of both the DWTPs and the pumping station,  $\text{ClO}_2^-$  was  $0.680 \text{ mg L}^{-1}$  and  $0.733 \text{ mg L}^{-1}$ , respectively, at the outlet of the east and west DWTP, and  $\text{ClO}_3^-$  was  $0.081 \text{ mg L}^{-1}$  and  $0.082 \text{ mg L}^{-1}$ , respectively, at the outlet of the east and west DWTP.

After inserting the initial disinfectant and DBP concentrations,  $\text{Cl}_2$ ,  $\text{ClO}_2^-$ , and  $\text{ClO}_3^-$  kinetics were defined in the model, assigning the reaction kinetic order and the  $k_b$  to each parameter. The order of the reaction kinetics and  $k_b$  inserted in the model for residual  $\text{Cl}_2$ ,  $\text{ClO}_2^-$ , and  $\text{ClO}_3^-$  were the ones determined at laboratory scale, respectively, for the residual  $\text{ClO}_2$ ,  $\text{ClO}_2^-$ , and  $\text{ClO}_3^-$ .

### Comparison between measured and simulated data

Different simulations of the residual  $\text{Cl}_2$ ,  $\text{ClO}_2^-$ , and  $\text{ClO}_3^-$  propagation in the DWDS were carried out on the modeled system. The pressure, flow, residual  $\text{Cl}_2$ ,  $\text{ClO}_2^-$  and  $\text{ClO}_3^-$  measured at different points of the system were compared

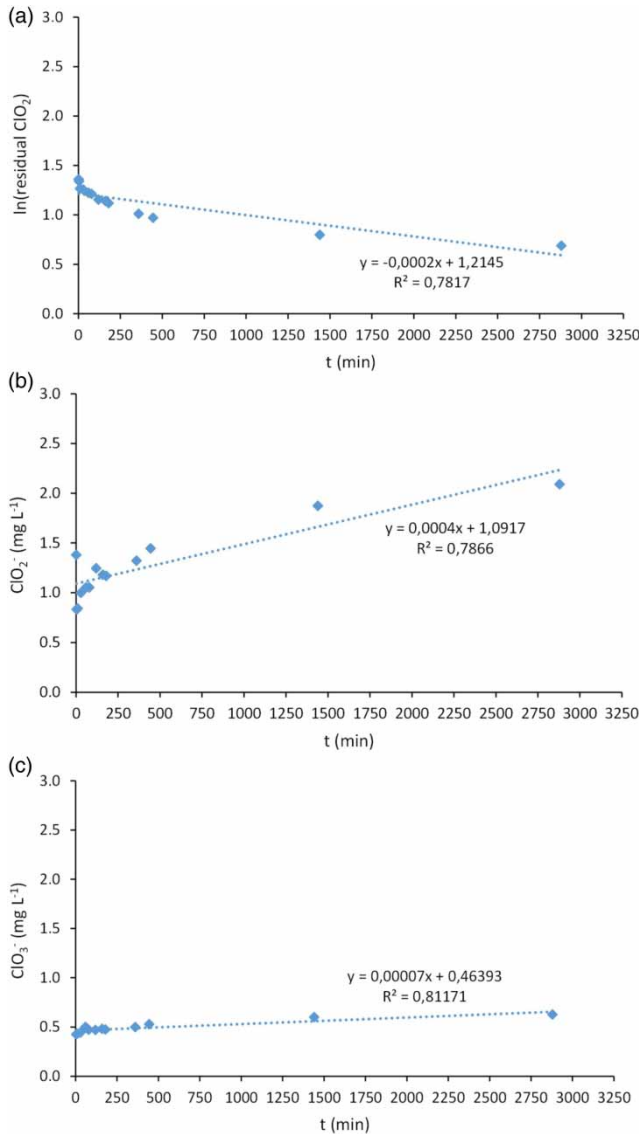


**Figure 6** |  $\ln(\text{Residual } \text{ClO}_2)$  (a),  $\text{ClO}_2^-$  (b), and  $\text{ClO}_3^-$  (c) versus time determined by batch experiments at laboratory scale for the determination of kinetic reactions. In each graph, the interpolation line is reported with the respective equation and correlation coefficient.

to the simulated values. The measured values were the average values measured at each sampling point of the system (Figure 1) at 10.00 a.m. during the monitoring campaign from 2006 to 2011 (see section ‘Evaluation of the disinfectant and DBP concentrations in the distribution system’). The simulated values were evaluated at the same sampling points (Figure 1) at 10.00 a.m. after one month from the start of the disinfectant dosing in the DWTPs in the

model. The period of one month was chosen because after one month a stable water quality condition was achieved in the model simulation.

### Analytical methods

The  $\text{ClO}_2$  residual concentration during the batch experiments was determined with a residual chlorine analyzer ( $\text{Cl}_2$  detection limit =  $0.05 \text{ mg L}^{-1}$ ) (APAT IRSA CNR 4080 2003). Since the chlorine analyzer measured the  $\text{Cl}_2$  concentration, the  $\text{ClO}_2$  concentration was calculated from the detected  $\text{Cl}_2$  values with a conversion factor:  $\text{ClO}_2 = 1.9 \text{ Cl}_2$ . The  $\text{ClO}_2^-$  and  $\text{ClO}_3^-$  concentrations were determined using Ion Chromatography Dionex ICS 5000 (detection limit  $\text{ClO}_2^- = 0.05 \text{ mg L}^{-1}$  and  $\text{ClO}_3^- = 0.03 \text{ mg L}^{-1}$ ) (UNI EN ISO 10304-4).

## RESULTS AND DISCUSSION

### Analysis of the residual chlorine, chlorite, and chlorate concentrations in the real distribution system

The residual  $\text{Cl}_2$ ,  $\text{ClO}_2^-$ , and  $\text{ClO}_3^-$  concentrations were analyzed at 26 points of the DWDS from 2006 to 2011 (Figure 7).

The results show that the residual  $\text{Cl}_2$  was always below the WHO GV of  $0.2 \text{ mg L}^{-1}$  and sometimes was absent (Figure 7(a)). This is a negative aspect, since the chlorine absence implies a null protection from bacterial contamination at these points of the DWDS, so water safety cannot be ensured.

The  $\text{ClO}_2^-$  concentration from 2006 to 2008 often exceeded the WHO GV of  $700 \mu\text{g L}^{-1}$ , in particular at the points of the system more distant from the DWTPs (Figure 7(b)). From 2009 to 2011, the  $\text{ClO}_2^-$  concentration was below the GV. The data showed significant variability before 2008, which subsequently decreased; this trend was probably due to the reduction of the  $\text{ClO}_2$  dosage in the DWTP after a gradual cleaning of the DWDS pipes in 2008. Overall, the  $\text{ClO}_2^-$  concentration exceeded the WHO GV for 12–16% of results in the first 2 years, for 48% of results in 2008, and for 1–8% of results from 2009 to 2011.

The  $\text{ClO}_3^-$  concentration was significantly below the WHO GV of  $700 \mu\text{g L}^{-1}$  throughout the monitoring period (Figure 7(c)).

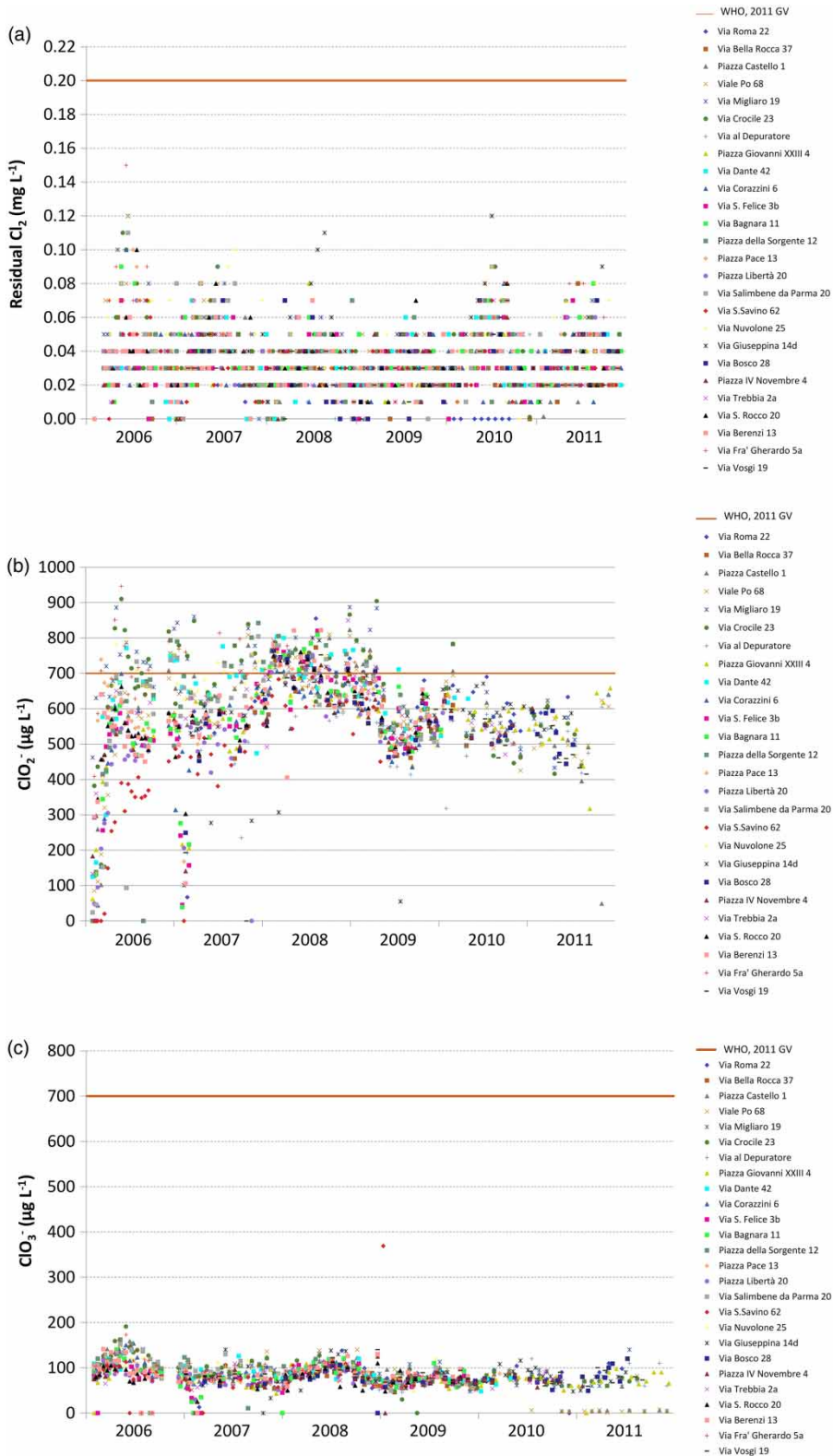


**Figure 7** | Residual  $\text{Cl}_2$  (a),  $\text{ClO}_2^-$  (b), and  $\text{ClO}_3^-$  (c) versus time measured in the distribution system of Cremona (Italy) from 2006 to 2011 (sampling point position is shown in Figure 1).

### Determination of the mixing zone

The simulations aimed at determining the water mixing zone showed that, dosing salt in the east DWTP and pumping station, a salt concentration diverse from zero in the modeled DWDS reached the junctions more distant from the east DWTP and from the pumping station for the first time at 6.00 a.m. and at 7.00 a.m. The salt concentration in the

modeled DWDS after 6 and 7 hours from the start of the salt dosing ( $70,000 \text{ mg L}^{-1}$ ) in the east DWTP is reported in Figure 8. After 6 and 7 hours, the farthest points of the DWDS reached by the salt were junctions a, c, e, g, h, and i.

Dosing salt in the west DWTP, a salt concentration diverse from zero in the modeled DWDS reached the junctions more distant from the west DWTP for the first time at 7.00 p.m. and at 11.00 p.m. The

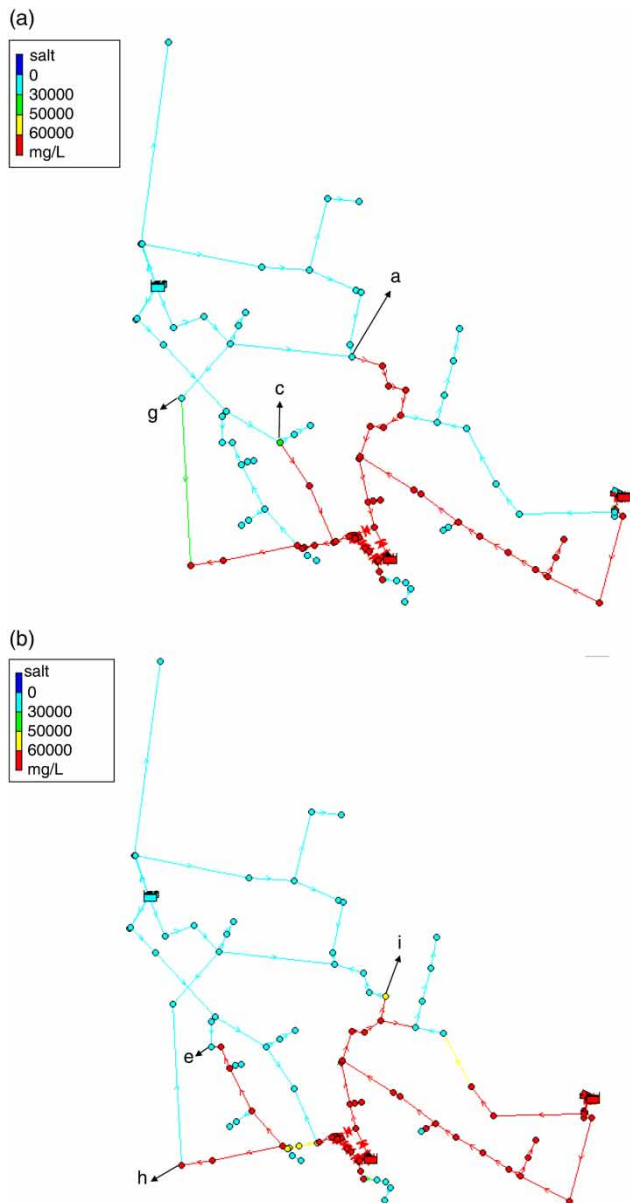


**Figure 8** | Salt concentration in the modeled DWDS after 6 (a) and 7 (b) hours from the start of the salt dosing in the east DWTP.

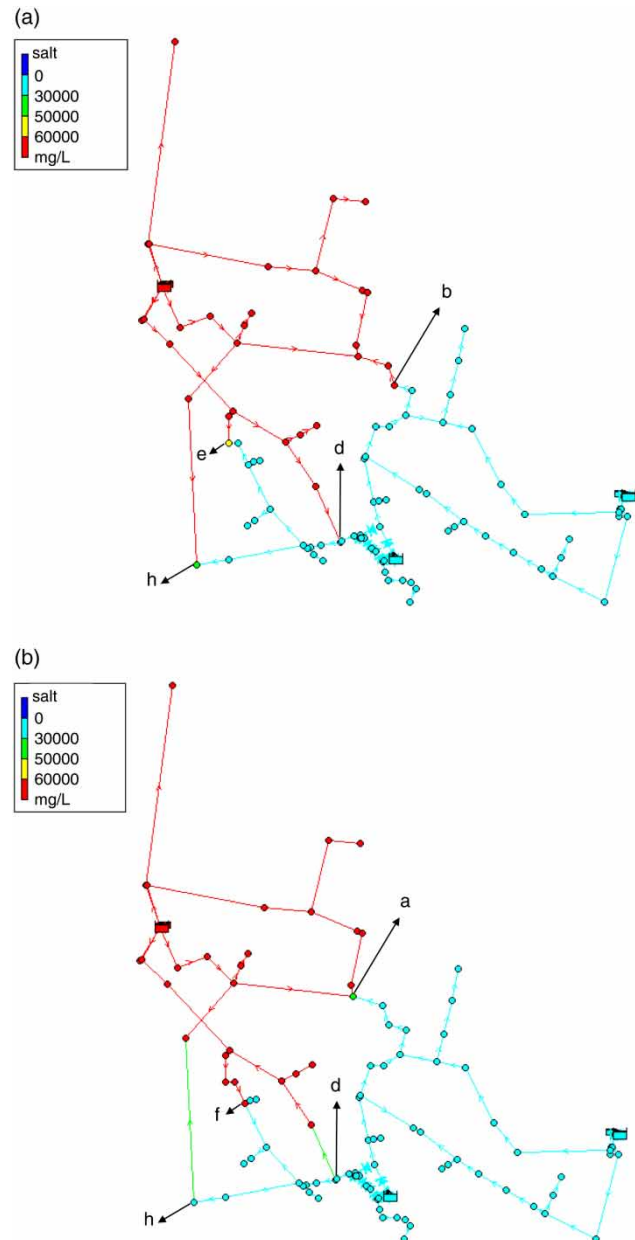


**Figure 9** | Salt concentration in the modeled DWDS after 19 (a) and 23 (b) hours from the start of the salt dosing in the west DWTP.

propagation of the salt was evaluated in the modeled DWDS after 19 and 23 hours from the start of the salt dosing ( $70,000 \text{ mg L}^{-1}$ ) in the west DWTP (Figure 9). After 19 and 23 hours, the farthest points of the DWDS reached by the salt were junctions a, b, d, e, f, and h.

The DWDS zone where water coming from the east and west DWTP is mixed was determined by comparing the results of the two simulations of the salt propagation (Figures 8 and 9). The mixing zone is constituted by the pipes of the DWDS between junctions a–b, c–d, e–f, and g–h (Figure 10).

### Residual chlorine, chlorite, and chlorate propagation in the modeled distribution system

The  $\text{Cl}_2$  residual in the modeled DWDS at 10 a.m. after one month from the start of the disinfectant dosing in both the DWTPs is reported in Figure 11(a). This time was chosen since the water sampling at the different points of the DWDS usually takes place at 10 a.m. for the laboratory analysis. The results of the residual  $\text{Cl}_2$  propagation modeling showed that the  $\text{Cl}_2$  residual

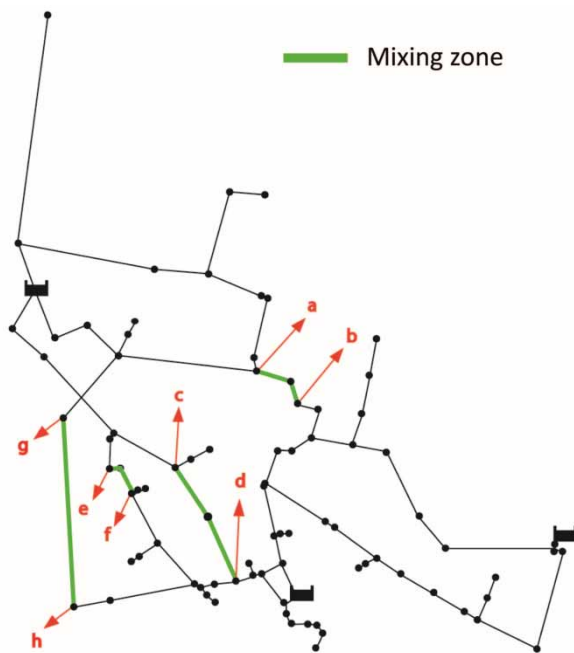


Figure 10 | Water mixing zone in the modeled DWDS determined with Epanet 2.0.

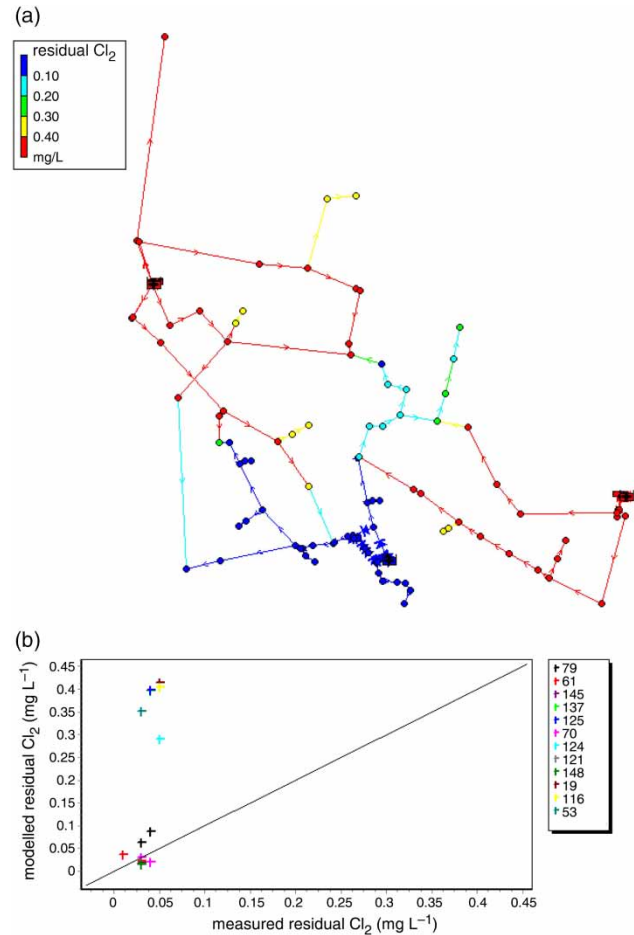


Figure 11 | Residual  $\text{Cl}_2$  in the modeled DWDS at h 10 a.m. after one month from the start of the disinfectant dosing in both the DWTPs (a); correlation between the measured and modeled residual  $\text{Cl}_2$  concentrations in the DWDS (b).

concentrations were still high at points near the two DWTPs ( $0.42 \text{ mg L}^{-1}$ ), due to a very slow disinfectant consumption; with an increase in the distance from the DWTPs, a sharp residual  $\text{Cl}_2$  decay was observed. Moreover, in the mixing zone of the DWDS the residual  $\text{Cl}_2$  concentrations were still high, while low values were registered in the peripheral pipes of the modeled system. Furthermore, since the residual  $\text{Cl}_2$  concentration at the central pumping station was low, low concentrations were observed at the near junctions.

The correlation between the measured and modeled residual  $\text{Cl}_2$  concentrations was evaluated (Figure 11(b) and Table 1). The model tends to overestimate the residual  $\text{Cl}_2$  concentrations in 67% of the cases, compared to the measured concentrations in the real DWDS. Considering

**Table 1** | Comparison between measured and modeled residual Cl<sub>2</sub> concentrations, mean absolute error, and root mean square error, at 10 a.m. after one month from the start of the disinfectant dosing in both the DWTPs

Junction number (sampling point)	Residual Cl <sub>2</sub> (mg L <sup>-1</sup> )		Mean absolute error	Root mean square error
	Measured	Modeled		
79	0.035	0.08	0.040	0.041
61	0.02	0.03	0.017	0.020
145	0.03	0.02	0.011	0.011
137	0.04	0.40	0.357	0.357
125	0.04	0.40	0.359	0.359
70	0.035	0.02	0.011	0.015
124	0.05	0.29	0.241	0.241
121	0.03	0.01	0.016	0.016
148	0.03	0.02	0.014	0.014
19	0.05	0.41	0.365	0.365
116	0.05	0.40	0.354	0.354
53	0.03	0.35	0.322	0.322

the root mean square error (Table 1), half the results showed a high error value (>0.100). This result can be due to the fact that the pipe wall effect was not evaluated in the simulation, because of the difficulty in simulating this effect at laboratory scale, while in the real system the additional reactions at pipe walls could influence water quality and, therefore, the disinfectant consumption. For instance, pipe material and biofilm in pipes could affect the water quality, determining a high ClO<sub>2</sub> consumption. Moreover, it is possible that in the real system, a residual contaminant in water (e.g., NOM) can react with the disinfectant, determining a higher ClO<sub>2</sub> consumption and, consequently, lower Cl<sub>2</sub> residual concentrations. These aspects, which were not evaluated in the model, should be further investigated in future studies.

The ClO<sub>2</sub><sup>-</sup> concentration in the modeled DWDS at 10 a.m. after one month from the start of the disinfectant dosing in both the DWTPs is reported in Figure 12(a). The results show that the ClO<sub>2</sub><sup>-</sup> concentrations at points near the two DWTPs were close to those from the outlet of the DWTPs (close to 0.70 mg L<sup>-1</sup>), since the ClO<sub>2</sub><sup>-</sup> formation was very slow; with an increase in the distance from the DWTPs, a gradual ClO<sub>2</sub><sup>-</sup> concentration increase was registered. Moreover, in the peripheral pipes and in the mixing zone of the

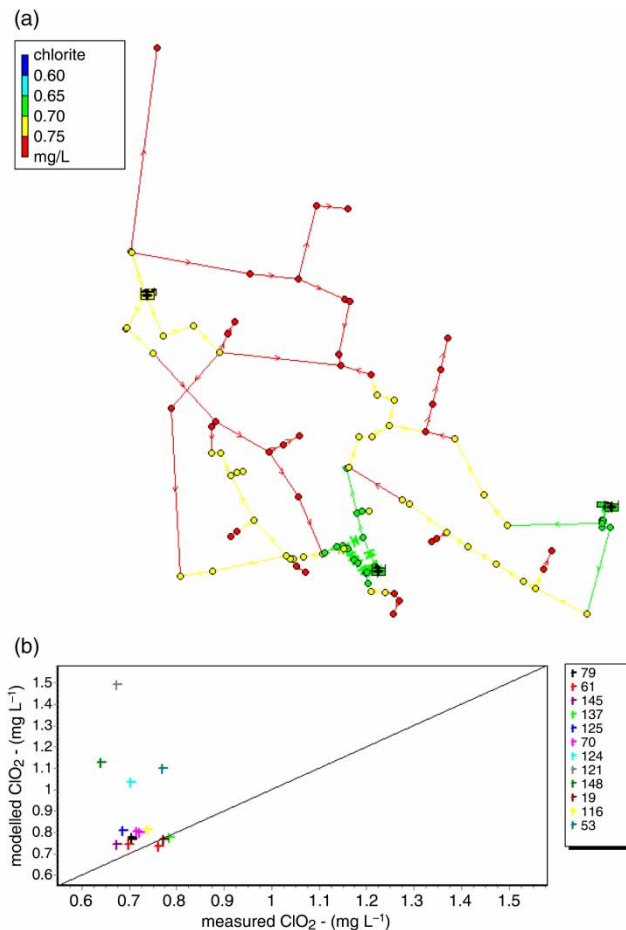


**Figure 12** | ClO<sub>2</sub><sup>-</sup> in the modeled DWDS at 10 a.m. after one month from the start of the disinfectant dosing in both the DWTPs (a); correlation between the measured and modeled ClO<sub>2</sub><sup>-</sup> concentrations in the DWDS (b).

modeled DWDS the ClO<sub>2</sub><sup>-</sup> concentrations were over the WHO GV of 700 µg L<sup>-1</sup>.

The correlation between the measured and modeled ClO<sub>2</sub><sup>-</sup> concentrations was evaluated (Figure 12(b)). The model tends to overestimate the residual ClO<sub>2</sub><sup>-</sup> concentrations in 75% of the cases, compared to the measured concentrations in the real DWDS. Considering the root mean square error (Table 2), only a few results showed a high error value (>0.100). As for the Cl<sub>2</sub> results, the differences between the modeled and measured ClO<sub>2</sub><sup>-</sup> concentrations were due to the aspects previously explained.

The ClO<sub>3</sub><sup>-</sup> concentration in the modeled DWDS at 10 a.m. after one month from the disinfectant dosing in both the DWTPs is reported in Figure 13(a). The results showed a

**Table 2** | Comparison between measured and modeled residual  $\text{ClO}_2^-$  concentrations, mean absolute error, and root mean square error, at 10 a.m. after one month from the start of the disinfectant dosing in both the DWTPs

Junction number (sampling point)	$\text{ClO}_2^-$ ( $\text{mg L}^{-1}$ )		Mean absolute error	Root mean square error
	Measured	Modeled		
79	0.704	0.770	0.068	0.069
61	0.730	0.740	0.036	0.037
145	0.674	0.740	0.070	0.070
137	0.784	0.780	0.008	0.008
125	0.686	0.810	0.123	0.123
70	0.719	0.800	0.084	0.085
124	0.703	1.030	0.331	0.331
121	0.673	1.490	0.820	0.820
148	0.640	1.130	0.486	0.486
19	0.772	0.770	0.007	0.007
116	0.738	0.810	0.074	0.074
53	0.769	1.100	0.331	0.331

very low  $\text{ClO}_3^-$  concentration gradient. Near the two DWTPs,  $\text{ClO}_3^-$  formation was negligible, since the concentrations were close to those from the outlet of the DWTPs (close to  $0.10 \text{ mg L}^{-1}$ ); with an increase in the distance from the DWTPs, a slow and gradual  $\text{ClO}_3^-$  concentration increase was observed, with values always below the WHO GV of  $700 \mu\text{g L}^{-1}$ .

The correlation between the measured and modeled  $\text{ClO}_3^-$  concentrations was evaluated (Figure 13(b)). As for  $\text{ClO}_2$ , the model tends to overestimate the residual  $\text{ClO}_3^-$  concentrations in 75% of the cases, compared to the measured concentrations in the real DWDS. Considering the root mean square error (Table 3), only one result showed a high error value ( $>0.100$ ). Also in this case, the differences between the modeled and measured  $\text{ClO}_3^-$  concentrations were probably due to the aspects previously explained.

## CONCLUSIONS

In this work the distribution system of Cremona, in the north of Italy, was monitored for 6 years (2006–2011) analyzing residual chlorine, chlorite, and chlorate concentrations. The USEPA software Epanet 2.0 was applied to the distribution network in order to simulate

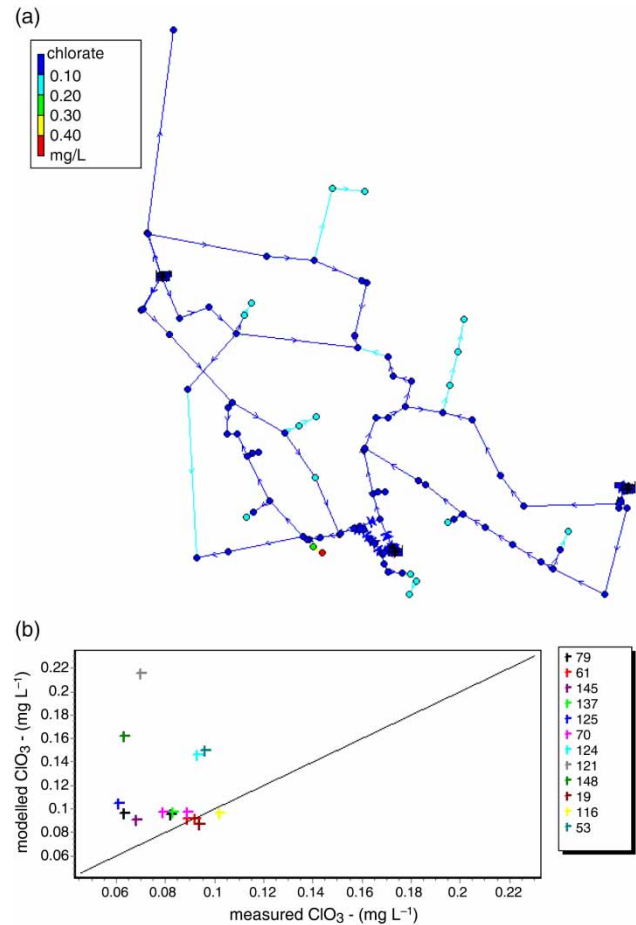


**Figure 13** |  $\text{ClO}_3^-$  in the modeled DWDS at 10 a.m. after one month from the start of the disinfectant dosing in both the DWTPs (a); correlation between the measured and modeled  $\text{ClO}_3^-$  concentrations in the DWDS (b).

the propagation of residual chlorine, chlorite, and chlorate, and in order to estimate the mixing zone of the water coming from the west and east treatment plants. The measured and simulated concentrations were compared.

The results of the network monitoring showed a high chlorine dioxide consumption and a significant chlorite formation. Predictably, this occurred mainly at the points of the network more distant from the treatment plants, where it exceeded the GV. Conversely, a low chlorate formation was registered. The propagation of chlorine and DBPs was simulated with the software, and the correlation was evaluated between the measured and the modeled results. Moreover, the water mixing zone in the distribution network was determined.

**Table 3** | Comparison between measured and modeled residual  $\text{ClO}_3^-$  concentrations, mean absolute error, and root mean square error, at 10 a.m. after one month from the start of the disinfectant dosing in both the DWTPs

Junction number (sampling point)	$\text{ClO}_3^-$ (mg L <sup>-1</sup> )		Mean absolute error	Root mean square error
	Measured	Modeled		
79	0.073	0.100	0.024	0.026
61	0.091	0.090	0.001	0.002
145	0.068	0.090	0.023	0.023
137	0.083	0.100	0.014	0.014
125	0.061	0.100	0.043	0.043
70	0.084	0.100	0.013	0.013
124	0.093	0.150	0.053	0.053
121	0.070	0.220	0.145	0.145
148	0.063	0.160	0.099	0.099
19	0.094	0.090	0.007	0.007
116	0.102	0.100	0.006	0.006
53	0.096	0.150	0.054	0.054

This study shows how  $\text{ClO}_2$ ,  $\text{ClO}_2^-$ , and  $\text{ClO}_3^-$  kinetic reactions determined at laboratory scale can be used to describe the rates of reaction of these compounds in the DWDS. However, the differences between some of the measured and modeled concentrations were probably due to the kinetic study carried out at the laboratory scale in batch conditions and to the pipe wall effect, which was not evaluated in this study because of the difficulty in simulating it at laboratory scale. Moreover, it is possible that in the real system, a residual contaminant in water (e.g., NOM) can react with the disinfectant, determining a higher  $\text{ClO}_2$  consumption and, consequently, lower  $\text{Cl}_2$  residual concentrations. Therefore, further modeling should be carried out to determine the chlorine and DBP reaction kinetics, considering the pipe wall effect, in order to optimize the model. Notwithstanding, the proposed model is a useful tool since it is personalized for the studied drinking water distribution network, as specific disinfectant and DBP kinetics for the water distributed were determined at laboratory scale and were applied to the specific system. The model has proved to be a useful instrument for the prediction of the disinfectant and DBP propagation in the drinking water distribution network and is a valid support for water utility management.

## ACKNOWLEDGEMENTS

The authors would like to thank Padania Acque Gestione SpA, which is the company that manages the drinking water supply system of Cremona (Italy) studied in this research. Special thanks also go to the company's technical staff who took part in this experimentation. Sabrina Sorlini planned and supervised the research activities and the paper drafting, Michela Biasibetti did the data analysis/simulation and took care of the paper draft; Francesca Gialdini contributed to the experimentation and Alessandro Muraca supervised the hydraulic aspects of the research activities.

## REFERENCES

- Al-Jasser, A. O. 2007 Chlorine decay in drinking-water transmission and distribution systems: pipe service age effect. *Water Research* **41** (2), 387–396.
- APAT IRSA CNR 4080 2003 Official Analytical Method Free Active Chlorine. <http://www.irsa.cnr.it/Docs/Capitoli/1000.pdf> (accessed 12 November 2016).
- Baribeau, H., Prévost, M., Desjardins, R., Lafrance, P. & Gates, D. J. 2002 Chlorite and chlorate ion variability in distribution systems. *Journal of American Water Works Association* **94** (7), 96–105. <http://www.jstor.org/stable/41298419>.
- Boano, F., Fiore, S. & Revelli, R. 2016 Chlorate formation in water distribution systems: a modeling study. *Journal of Hydroinformatics* **18** (1), 115.
- Clark, R., Grayman, W. M., Males, R. M. & Hess, A. F. 1993 Modeling contaminant propagation in drinking-water distribution systems. *Journal of Environmental Engineering* **119** (2), 349–364.
- Clark, R., Grayman, W., Goodrich, J., Deining, R. & Skov, K. 1994 Measuring and modeling chlorine propagation in water distribution systems. *Journal of Water Resources Planning and Management* **120** (6), 871–887.
- Collivignarelli, C. & Sorlini, S. 2004 Trihalomethane, chlorite and bromate formation in drinking water oxidation of Italian surface waters. *Journal of Water Supply: Research and Technology-Aqua* **53** (3), 159–168. <http://aqua.iwaponline.com/content/53/3/159.abstract> (accessed 12 November 2016).
- Courtis, B. J., West, J. R. & Bridgeman, J. 2009 Chlorine demand-based predictive modeling of THM formation in water distribution networks. *Urban Water Journal* **6** (6), 407–415.
- Gates, D., Ziglio, G. & Ozekin, K. 2009 *State of the Science of Chlorine Dioxide in Drinking Water*. Water Research Foundation and Fondazione AMGA, Genoa, Italy.
- Islam, M., Chaudhry, M. & Clark, R. 1997 Inverse modeling of chlorine concentration in pipe networks under dynamic

- condition. *Journal of Environmental Engineering* **123** (10), 1033–1040.
- Kiéné, L., Lu, W. & Lévi, Y. 1998 Relative importance of the phenomena responsible for chlorine decay in drinking water distribution systems. *Water Science and Technology* **38** (6), 219–227.
- Korn, C., Andrews, R. C. & Escobar, M. D. 2002 Development of chlorine dioxide-related by-product models for drinking water treatment. *Water Research* **36** (1), 330–342.
- Lafrance, P., Duschene, P., Arcouette, N. & Prevost, M. 1992 The use of ClO<sub>2</sub>: case study of Laval. In: *Proceedings of the Second International Symposium on Chlorine Dioxide*, 7–8 May, Houston, TX, USA.
- Legislative Decree n. 31 2001 Execution of Directive 98/83/CE Related to Drinking Water Quality.
- Li, X. & Zhao, H. 2006 Development of a model for predicting trihalomethanes propagation in water distribution systems. *Chemosphere* **62** (6), 1028–1032.
- McGuire, M. J., Krasner, S. W. & Stevens, A. A. 1990 Nature and occurrence of disinfection by-products in the United States. In: *Proceedings 2nd Japan – US Governmental Conference on Drinking Water Quality Management*, Tokyo, Japan.
- Mohamed, H. I. & Abozeid, G. 2011 Dynamic simulation of pressure head and chlorine concentration in the city of Asyut water supply network in abnormal operating conditions. *Arabian Journal for Science and Engineering* **36** (2), 173–184.
- Olivieri, V. P., Snead, M. C., Krusé, C. W. & Kawata, K. 1986 Stability and effectiveness of chlorine disinfectants in water distribution systems. *Environmental Health Perspectives* **69**, 15–29. <http://www.ncbi.nlm.nih.gov/pmc/articles/PMC1474301/> (accessed 12 November 2016).
- Rodriguez, M. J. & Sérodes, J. B. 1998 Assessing empirical linear and non-linear modelling of residual chlorine in urban drinking water systems. *Environmental Modelling & Software* **14** (1), 93–102.
- Rodriguez, M. J. & Sérodes, J. B. 2001 Spatial and temporal evolution of trihalomethanes in three water distribution systems. *Water Research* **35** (6), 1572–1586.
- Rossmann, L. A. 2000 *Epanet 2.0 User's Manual*. United States Environmental Protection Agency, Washington, DC, USA.
- Rossmann, L. A., Clark, R. M. & Grayman, W. M. 1994 Modeling chlorine residuals in drinking-water distribution systems. *Journal of Environmental Engineering* **120** (4), 803–820.
- Sadiq, R. & Rodriguez, M. J. 2004 Disinfection by-products (DBPs) in drinking water and predictive models for their occurrence: a review. *Science of the Total Environment* **321** (1–3), 21–46.
- Sarin, P., Snoeyink, V. L., Bebee, J., Kriven, W. M. & Clement, J. A. 2001 Physico-chemical characteristics of corrosion scales in old iron pipes. *Water Research* **35** (12), 2961–2969.
- Sarin, P., Snoeyink, V. L., Bebee, J., Jim, K. K., Beckett, M. A., Kriven, W. M. & Clement, J. A. 2004a Iron release from corroded iron pipes in drinking water distribution systems: effect of dissolved oxygen. *Water Research* **38** (5), 1259–1269.
- Sarin, P., Snoeyink, V. L., Lytle, D. A. & Kriven, W. M. 2004b Iron corrosion scales: model for scale growth, iron release, and colored water formation. *Journal of Environmental Engineering* **130** (4), 364–373.
- Thompson, A. L. 1988 Chlorite and chlorate residuals in the distribution system. In: *Proceedings 1988 AWWA WQTC*, St Louis, MO, USA.
- UNI EN ISO 10304-4. 2001 Water quality. Determination of dissolved anions by ion chromatography in liquid phase. Determination of chlorates, chlorides and chlorites in water with a low level of contamination. [http://www.iso.org/iso/iso\\_catalogue/catalogue\\_tc/catalogue\\_detail.htm?csnumber=22573](http://www.iso.org/iso/iso_catalogue/catalogue_tc/catalogue_detail.htm?csnumber=22573) (accessed 12 November 2016).
- Wable, O., Dumoutier, N., Duguet, J. P., Jarrige, P. A., Gelas, G. & Depierre, J. F. 1991 Modelling chlorine concentrations in a network and applications to Paris distribution network. Water quality modeling in distribution systems. In: *Proceedings of the American Water Works Association Research Foundation Conference, Water Quality Modeling in Distribution Systems*, Cincinnati, OH, USA, pp. 265–276.
- WHO 2011 *Guidelines for Drinking Water Quality*, 4th edn. World Health Organization, Geneva, Switzerland.
- Zhang, G. R., Kiéné, L., Wable, O., Chan, U. S. & Duguet, J. P. 1992 Modelling of chlorine residual in the water distribution network of Macao. *Environmental Technology* **13** (10), 937–946.
- Zhang, Z., Stout, J. E., Yu, V. L. & Vidic, R. 2008 Effect of pipe corrosion scales on chlorine dioxide consumption in drinking water distribution systems. *Water Research* **42** (1–2), 129–136.

First received 20 January 2016; accepted in revised form 10 August 2016. Available online 19 October 2016